Power Over Fiber Pooling as Part of 6G Optical Fronthaul

C. Vázquez, *Senior Member, IEEE*, G. Otero, R. Altuna, J. D. López-Cardona, and D. Larrabeiti, *Member, IEEE*

***Abstract*—Key parameters required in 5G advanced networks are higher peak data rates, lower latency but with improved energy efficiency. Those key performance indicators are further pushed forward in the envisioned 6G requirements, among others in achieving real energy efficiency by providing broadband low power communications with efficient powering strategies. Power over fiber (PoF) Pooling in centralized radio access networks with optical switching provides energy aware device control and resource allocation capabilities. Algorithms to implement PoF pooling with different types of optical fibers and supported by battery charge at remote radio heads are developed in a phantom cell scenario showing throughput enhancement while optimizing power consumption. Experiments as proof of concept are performed using a 4×4 optical switch at central office optically feeding various RRHs with different power requirements through single mode fiber links of up to 15 km and supported by a bidirectional communication link. The RRH deep sleep mode consumes 5.8 mW. A mobility manager emulates users' mobility within cells and allows the optimized selection of the awaken cells considering energy efficiency and traffic throughput. Some tests with different multicore fibers are also performed.**

***Index Terms*—5G, 6G, battery charge, energy efficiency, mobile communications, optical fibers, optical switches, photovoltaic power converters, power lasers, power over fiber, radio access networks.**

I. Introduction

THE 5G era increases the performance of the network by not only the growth of bandwidth and reduction of latency but also the ability to service numerous devices. Meaning that many issues arise which determine a non-linear growth of the energy consumption [1]. In 6G ecosystems, energy efficiency is another relevant consideration besides frequency when designing the transmission system [2]. No standardized framework has been established for 6G mobile communications as of now. On December 4, 2023, 3GPP issued a press release [3], expressing readiness to shape the future of 6G drawing from its extensive experience in developing specifications for 3G, 4G, and 5G technologies. Despite the absence of a formal standard, the progression of Key Performance Indicators (KPIs) from 5G to 6G has been a subject of extensive discourse. [2] and [4] provide insights into anticipated KPI evolution in the transition from 5G to 6G. To prevent a significant overall rise in power consumption compared to 5G, a targeted $\times 300$ improvement in energy efficiency is envisaged for 6G. This enhancement, defined as power per bit/s, aligns with the projected $\times 10$ growth in average data rate, resulting in a potential net power saving of $\times 30$ in 6G if the target KPIs are achieved. The employment of smaller cells in 6G to achieve higher rates suggests reduced individual power requirements per cell. Optical fibers high bandwidth and ubiquity provide ideal features in advanced 5G/6G radio access networks (RAN), as part of the back/front haul infrastructure for transmitting radio–over-fiber (RoF) signals. The Cloud-RAN (C-RAN) architectures centralize the computing power, share resources and simplify the management of the mobile network [5]. Adding energy management to the central office can help in sharing power dissipation and improving the overall power management. Heterogeneous C-RAN networks are good candidates with high data rate, minimized interference and improved energy efficiency, by including energy harvesting and maximizing resource allocation and power allocation [6]. The cell size of remote radio heads (RRH) will become smaller by increasing the carrier frequency of RF signals, because RF signals with a higher carrier frequency have higher wireless transmission loss. They can be integrated in a phantom-cell architecture, where the traditional Base Stations (BS) overlays with low-power, low-cost and high-bandwidth access nodes called femtocells [7].

ARoF (Analog Radio over Fiber) is a technique used to transmit analog radio frequency signals over a fiber optic network. With ARoF, the RF signal is converted into an optical signal, which is transmitted through the fiber optic cable and then converted back into an RF signal at the receiver. This technique is used in high-frequency radio applications such as broadcasting, mobile telephony, and radio determination. On the other hand, DRoF (Digital Radio over Fiber) is a technique used to transmit digital signals over a fiber optic network. With DRoF, the digital signal is modulated into an optical signal, which is transmitted through the fiber optic cable and then demodulated back into a digital signal at the receiver. This technique is used in high-speed

Manuscript received 3 November 2023; revised 15 January 2024 and 6 March 2024; accepted 7 March 2024. Date of publication 18 March 2024; date of current version 16 July 2024. This work was supported in part by Ministerio de Asuntos Económicos y Transformación Digital European Union—NextGeneration EU/PRTR under Grant TSI-063000-2021-135 and Grant TSI-063000-2021-137, and in part by Agencia Estatal de Investigación-Ministerio de Ciencia e Innovación under Grant PID2021-122505OB-C32. *(Corresponding author: C. Vázquez.)*

C. Vázquez, R. Altuna, and J. D. López-Cardona are with the Electronics Technology Department, Universidad Carlos III de Madrid, 28911 Leganés, Spain (e-mail: cvazquez@ing.uc3m.es).

G. Otero and D. Larrabeiti are with the Telematics Department, Universidad Carlos III de Madrid, 28911 Leganés, Spain.

Color versions of one or more figures in this article are available at https://doi.org/10.1109/JLT.2024.3375972.

Digital Object Identifier 10.1109/JLT.2024.3375972

fiber optic communication network applications such as long-distance data transmission and data center interconnection.

In future 5G C-RAN architectures, simplified RRH will be present, especially when using ARoF technologies sending RF signals that are ready for antenna transmission with no need of a high-speed digital-to-analog and analog-to-digital conversion with the consequent reduction in power consumption while making a better use of the large available bandwidth thus providing a greater throughput [8]. Some proposals of future elements on those RRHs include new photodetectors (PD) in the range from 23.5–31.5 GHz with low noise amplifiers [9] and UTC-PD working at 92 GHz [10], with power consumptions of 160 mW and 50 mW, respectively. By integrating ARoF and DRoF techniques with other technologies such as Power over Fiber (PoF), more energy-efficient and cost-effective communication networks can be created. RoF and PoF synergies can be exploited to further improve energy efficiency by adding a PoF layer to the RoF fronthauling. The new PoF layer can support sleep mode operation in RRHs with low power consumptions during idle periods [11]. PoF allows providing energy to remote nodes free of electromagnetic interference, with low weight, good galvanic isolation and with an easy integration in the front haul infrastructure of telecommunication operators. PoF is part of the technologies considered for future 6G RAN small cells in [12]. The capacity to feed 150 W in a double-clad fiber (DCF) [13] includes the use of the first multimode cladding to deliver the energy, meanwhile the data, which in this case does not comply with the 5G-NR standard, propagates through the single-mode core. In other case, the optical fronthauling transmitting 5G-NR signals uses single mode fibers (SMF) and the energy to feed the power amplifier (PA) required to achieve good quality signal, meaning EVM values within the 5G-NR standard [14], is delivered through multimode fibers (MMF) [15]. The set-up includes sleep mode operation capabilities to reduce RRH power consumption. All those configurations deliver the energy at distances from 100 m to 1 km, but they cannot reach longer distances without a high penalty in the overall PoF system efficiency because of the high optical fiber attenuation at the high power laser (HPL) central wavelength of around 800 nm. Meanwhile, photovoltaic power converter (PPC) efficiencies have still room for improvement [16]. In comparison with SMF, Multicore fibers (MCF) are used for higher power delivery, achieving more than 11 W at the reception stage; however reaching no more than 1 km by using a wavelength of 1064 nm [17]. PoF systems achieving longer distances of more than 10 km and including sleep mode and/or control capabilities are reported for SMF in [11] and for 7 uncoupled-core MCF in [18]. In those cases, the non-linear effects need to be analysed, especially in shared scenarios to avoid undesirable noise transfer of HPL instabilities to data channel [19], [20] and Stimulating Brioullin Scattering (SRS) if using a narrow linewidth HPL [21]. Those lengths are suitable for C-RAN front hauls using RoF. Spatial Division Multiplexing (SDM) using bundles of optical fibers or MCF and different switching capabilities in combination with PoF are alternatives in a multibeam antenna [22] with the beamformer kept at the Central Office (CO).

Different strategies based on a C-RAN architecture, knowing traffic loads and using different sleep mode configurations showed improvements of a 40% reduction of power consumption per day [23]. The 3rd Generation Partnership Project (3GPP) NR specification provides support for further enhance those enabling technologies that help reduce energy consumption at the RAN level such as 5G sleep modes [24]. Partial shutdown can also provide great savings, knowing that power amplifier consumes around 30% of RRH power consumption according to the power model provided in [25].

Regarding the consumption of current base stations, [26], [27] report power consumption at full load ranging from 6 W for femto base stations to 1 kW for macro base stations, based on data up to 2018. In light of 6G's goal for an $\times 30$ improvement in net power savings, it would mean a potential future power consumption of 0.2 W. Without batteries, PoF by itself can feed several types of femtocells. Other low power radio cells feature different powering levels depending on the operation mode [28]. Power consumptions for each radio range from as low as 100 mW to around 1 W, depending on if they are either single/dual band, number of MIMO channels and multiplexing type. In this context, other energy efficient proposals include the PoF pooling concept that allows sharing optical energy between different RRHs, depending on battery status and traffic demand [29], through a SDN controller. Preliminary tests on the control plane and integrated in a platform with ARoF were performed in [30].

In this paper, we describe algorithms supporting PoF pooling to provide energy aware device control and resource allocation capabilities. The implementation allows working with different types of optical fibers and integrates battery charge at RRHs. A scalable solution is developed for a MxN architecture. It is tested in a phantom cell scenario showing throughput enhancement while optimizing power consumption. A mobility manager emulates users' mobility within cells and allows the optimized selection of the awaken cells considering energy efficiency and traffic throughput. Some experiments as proof of concept are reported using a 4×4 optical switch at CO optically feeding several RRHs with different power requirements through various types of fibers and supported by a bidirectional communication link. In summary, we add the novel capability of having a pool with a limited number of lasers to dynamically provide power over fiber to a high number of remote nodes with batteries in combination with the development of an algorithm to have the maximum efficiency by distributing the energy smartly according to the location of the users in real time. The paper is organized as follows. In Section II, we describe the PoF pooling configuration integrated in the C-RAN architecture, the algorithms and the mobility manager with simulations developed to validate the PoF pooling concept. Section III describes the experimental setup for evaluating the performance of the PoF pooling functionality and delivering of PoF in the SDM approach including communications, and control. Section IV concludes the paper.

II. PoF Pooling Concept, System Model and Simulations

PoF pooling is a technique used in communication network systems that involves sharing a set of HPLs to provide electrical power to multiple devices in the network through optical

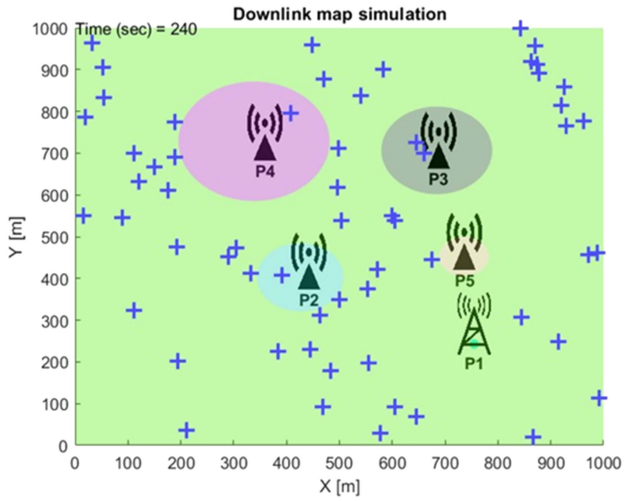

Fig. 1. Phantom cell scenario with one macrocell (P1) and four smallcells (P2-P5).

fiber [29]. Instead of using a separate power source for each device, a set of M lasers is used to power N devices simultaneously, with M<N, reducing the amount of equipment required and facilitating network management. In shared scenarios [21], PoF pooling utilizes Wavelength Division Multiplexing (WDM), which allows for multiple signals of different wavelengths to be transmitted through a single optical fiber. This enables the simultaneous transmission of data and energy through the same fiber. In PoF pooling, HPLs are used to power remote devices such as mobile network base stations or IoT devices through the optical fiber [19]. The lasers are controlled by a power management system that distributes the power according to the needs of each device in the network.

The energy allocation algorithm operates utilizing centralized information gathered from all femtocells. The algorithm takes into consideration the battery levels of each femtocell and makes real-time decisions on recharging, provided there are available lasers in the laser pool. The primary criterion for selecting a femtocell for recharging is straightforward: the algorithm prioritizes recharging the femtocell with the lowest battery level. This approach proves particularly beneficial as it allows us to leverage periods when femtocells are idle to recharge batteries, preparing for future instances of more intensive usage. By capitalizing on idle moments, the algorithm enhances overall network resilience and ensures optimal energy utilization for sustained performance.

PoF pooling offers several advantages, including reduced infrastructure costs, increased energy efficiency, and improved network management. Additionally, by using optical fiber instead of copper cables, electromagnetic interference is reduced, and data transmission security is enhanced.

Phantom cells are used in mobile networks to enhance efficiency and communication quality. These cells are small coverage areas that overlap with the main macro cells in a telecommunications network. The purpose of phantom cells is to allow mobile devices to connect to the cell with the strongest available signal, thereby reducing traffic in the macro cells and improving communication quality and speed. Although the femtocells used to create these phantom cells may or may not be available depending on the power situation, they are not essential elements for the operation of network communications. In fact, the purpose of phantom cells is to make communications more effective (achieve a higher rate and free up macro cells from their traffic) and more efficient (as appropriate for shorter transmission distance).

The macrocells and the associated phantom cells are part of a C-RAN architecture with centralized management. The controlled and planned resources include those to implement energy efficiency strategies such as powering through PoF. PoF adds value to most network technologies that will be used to complement the existing power system at RRH or to power battery-supported femtocells in a phantom cell scenario [29].

PoF algorithms should not interfere with the results of communication resources such as DRoF or ARoF, and they should strive to make the most of resources left by data channels.

A. System Model

Simulation appears to be the appropriate approach for planning a specific geographical implementation of PoF. In this work, we have further developed a tool [29] to simulate and visualize the performance of PoF in a phantom cell deployment, which includes multiple moving users in a geographical area sample. The tool calculates both the overall system performance and the energy efficiency achieved through the presence of femtocells with availability dependent on PoF and battery support. Fig. 1 provides an overview of the simulation tool for the PoF system. The positions of all base stations within the considered area are randomly chosen, following a Poisson Point Process (PPP). Then, the coverage maps for each base station are computed. Focusing on the downlink topology, it considers both the distance to the user and the transmission power from a macrocell or femtocell. This leads to weighted Voronoi cells. The observed differences in radii among the femtocells in the figure stem from our use of Weighted Voronoi tessellations [31] to compute coverage maps and influence areas. Weighted Voronoi maps make use of circles of Apollonius to consider both the transmission powers of base stations and the spatial arrangement between them. The coverage areas are intricately influenced by the proximity and power differentials between neighboring cells. Finally, the users, represented by blue crosses, are dropped onto the map and they start moving according to a random walk mobility model. The suitability of this approach has already been studied in [32], [33], [34]. To calculate the value of this performance indicator, we have modeled the wireless connection between users and base stations. For this purpose, the implemented signal model assumes that transmitted power decreases as a function of distance. Interferences between cells are also considered. However, some form of orthogonal time/frequency transmission (e.g., TDMA, OFDMA, etc.) is used within a cell to divide the uplink/downlink transmission spectrum into non-overlapping channels, ensuring no intracell interference.

Let ϕ_i be the PPP that models the location of the base stations at level i, and x_0 defines the location of the serving base station.

TABLE I
SIMULATION PARAMETERS

Area of Interest	1000 m x 1000 m
Base Stations	1 Macrocells 4 Femtocells 60 Users [37]
Radiated Power and bandwidth [27], [32], [38].	Macrocells → 46 dBm, 20 MHz Femtocells → 20 dBm, 1 GHz User devices → 20 dBm
Path-loss Exponent	4
RF Noise Level	-106 dBm
Femtocell Power Consumption	ON state → 0.96 W SLEEP state → 0.006 W
Available HPLs/Switch	One 5 W HPL One 1x4 Switch
Femtocell Battery Capacity	3300 mAh, [2.8 V - 3.3 V]

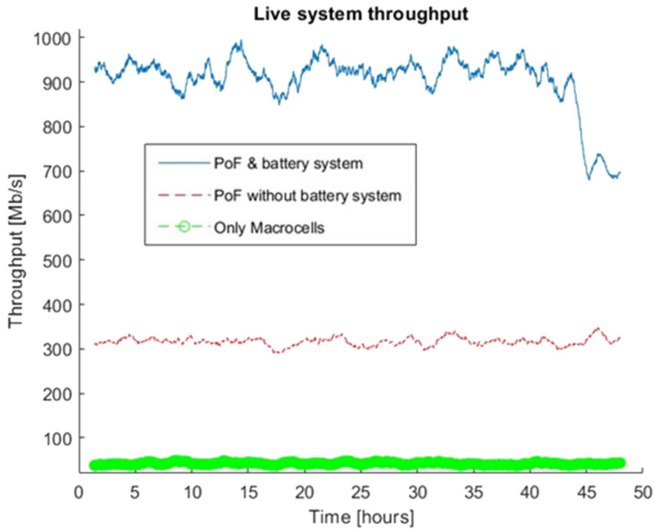

Fig. 2. Evolution of system throughput with the three strategies.

The final signal-to-interference-plus-noise ratio (SINR) of the downlink transmission is calculated for each user located at position y as follows [35] :

$$SINR^{-}(y) = \frac{P_i h_{x_0} ||x_0 - y||^{-\alpha}}{\sum_{j=1}^{k} \sum_{x \in \phi_i,\ x \neq x_0} P_j h_{x_0} ||x - y||^{-\alpha} + \sigma^2} \tag{1}$$

where P_i is the transmission power of the user, P_j is the transmission power of each interferer, h_{x_0} describes the Rayleigh fading attenuation, α is the path loss exponent, x and y are the positions of the interferer stations and the user device, respectively. Finally, σ^2 is the power of additive white Gaussian noise. The same reasoning applies to the uplink. Then, the final per-user performance in the downlink is calculated using the previously computed SINR as:

$$\begin{aligned} r_u^- &= \log_2\left(1 + SINR^-(u)\right) \\ r_u^+ &= \log_2\left(1 + SINR^+(u)\right) \end{aligned} \tag{2}$$

where r_u^- and r_u^+ are the downlink and uplink maximum achievable data rate, respectively, for a given user.

Bandwidth allocation among users of a cell is facilitated, contingent on a specific minimum power availability, which can be sourced from Power over Fiber, the femtocell's battery, or a combination of both. Our allocation approach involves employing a continuously differentiable, monotonically increasing, and strictly concave utility function, specifically a logarithmic function. Different studies [36] prove that under this logarithmic utility functions, an equitable distribution of resources among users leads to optimal resource allocation.

B. Simulation Scenario

Table I summarizes some of the most important parameters that determine the simulation scenario. It is worth noting that we consider a number of available HPLs in the pool that is less than the total amount of femtocells that could be a target for remote powering via the PoF technology. Note 0.96 W femtocell power consumption is an intermediate value from expected $\times 30$ net power energy savings that aligns with anticipated advancements in 6G's energy efficiency goals.

All the network elements (macrocells, femtocells, and users) are positioned into the area of interest and the simulation can start. Each femtocell's battery can be strategically recharged using the surplus power budget during periods of inactivity. We propose the following operational approach: when a device enters a femtocell's coverage area, it is accommodated by the femtocell under two conditions: 1) if an HPL is idle or 2) the femtocell's battery is available for use. In all other cases, the device is directed to the nearest Macro Base Station (MBS) for service. For this scenario, a custom temporal simulation was developed using MATLAB. Users are deployed on the map and start the movement.

Fig. 2 illustrates the overall system throughput over a continuous 24-hour period of user requests. We show the overall performance of the system's downlink as users move around the area of interest. As it can be noted in the figure, we compare three different alternatives regarding the utilized resources and management of energy: 1) a system where only macrocells are used (green dotted line), 2) a system with PoF with no batteries (red dashed line), and 3) a system including both PoF and the support of batteries (blue continuous line).

It's important to emphasize that the performance is significantly improved when utilizing a battery system compared to a battery-less system. This enhancement is attributed to the ability to activate more femtocells (N) than the number of lasers (M) when each base station is equipped with an integrated battery. It is particularly interesting the gradual convergence of throughput in the system incorporating both PoF and batteries toward the performance of the battery-less system, as the energy levels in the batteries deplete. Nevertheless, it's evident that smart energy management, such as utilizing PoF to recharge the batteries during periods of inactivity or during the night, has the potential to extend the operational lifespan of the batteries.

Finally, the simulator also computes the battery charge states of all femtocells in order to assess the behavior of the

system when utilizing the battery assisted alternative. This battery charge defines the remaining available service time for each femtocell when no lasers are available. Four different states are defined for each battery: a) no PoF charging, and femtocell is idle, b) no PoF charging, and femtocell is being used, c) PoF charging and in use, and d) PoF charging and not in use. Depending on the state of a specific femtocell, the battery will discharge at a faster or slower pace. A linear model to simulate battery discharge is considered as a first approximation.

Depending on the chosen values for different parameters, such as the power consumption of femtocells, laser power, or fiber attenuation, the system can transition from being energy-deficient to having a surplus or reaching a stable state. Additionally, other factors come into play when calculating the system's performance and consumption, such as user movement and their concentration in specific areas. It is worth noting that the simulator averages an adequate number of scenario repetitions to mitigate the impact of user movement randomness on the average results.

III. Real Set-Up and Proof of Concept

The testbed envisions to have a CO connected through a RoF optical front-haul to several small cell sites that can be partially powered by light and providing management functionalities at the CO including switching capabilities to select where to deliver the optical energy from a specific set of RRHs. This control functionality can be local or integrated in a SDN/NFV platform [30].

We have an experimental setup that integrates PoF modules as those described in [11], [18] using SMFs and another one using MCF. In all cases, they provide energy controlled from the CO, to allow the RRHs to enter into a sleep mode operation independently of the main power network and it also provides energy directly to the antenna or to recharge a battery. The minimum power consumption of each RRH corresponds to a deep sleep mode configuration that consumes 5.8 mW. There is a bidirectional communication from CO to RRHs including a channel at 1530 nm (downlink) and a channel at 1310 nm (uplink) to provide control from CO to RRH and send data from RRH to CO. The minimum active RRH power consumption including communications is around 70 mW [11].

The setup based on SMFs integrates a 4×4 high power optical switch (SW) in the CO that is controlled through a PoF agent that can be connected to a fronthaul SDN controller [30] and includes the mobility manager as part of the PoF pooling algorithm, see Fig. 3. It has been used to control the feeding of the set of 3 RRHs implemented, with only 1 or 2 RRHs receiving optical feeding. Bidirectional communication links, control, and communications (COM) boards [11] are deployed but not depicted. The PoF pooling concept requires switching between different RRHs to share the same HPLs at the CO for optimizing the resources allocation. There is a pool of 2 high power sources with around 2.2 W each at CO (implemented by splitting in 2 the output power of a 5 W Raman fiber laser at 1480 nm) to share between 4 outputs depending on the control signal, as in the PoF pooling concept. Fig. 4 shows four of the

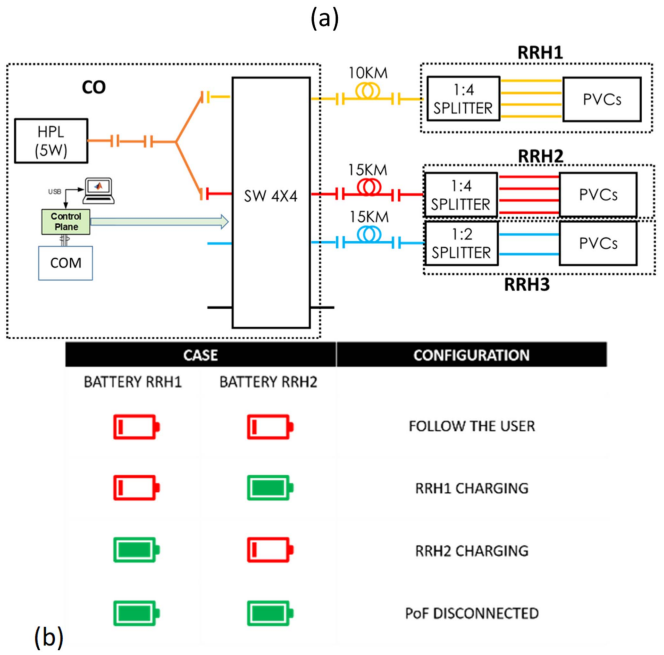

Fig. 3. (a) Simplified schematic of the PoF pooling system testbed with SMFs. SW = optical switch PVC = PPC = photovoltaic power converter. HPL = High Power Laser. COM = Communication board (b) functionality operation to test PoF pooling with mobility manager integration in testbeds.

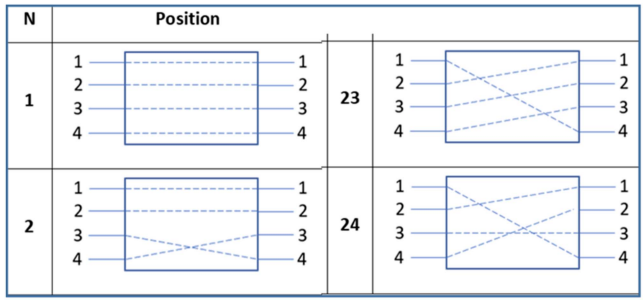

Fig. 4. Examples of 4×4 high power optical switch configurations.

24 available configurations of the Agiltron 4×4 SW that can handle up to 5 W.

The integration with the mobility manager allows to select the RRHs to awake depending on the traffic demand on a cell. Details about how this mobility manager works are described in Section II. In this setup, we tested the PoF pooling concept with an application in Matlab integrating mobility manager along with other functionalities and showed its scalability potential. An example of the operation with 2 RRHs is shown in Fig. 3(b). If both RRHs have low battery levels PoF energy feeds the RRH with a user, if only a battery level is below the threshold, then PoF feeds that RRH and PoF is disconnected if both batteries are charged. RRHs includes a 1×4 splitter to accommodate the maximum optical power that each photovoltaic power converter (PPC) can stand for.

HPL output of 37.5 dBm in PoF set-up supplies optical powers of 720 mW for RRH1 and 475 mW for RRH2 (see Fig. 3(a)).

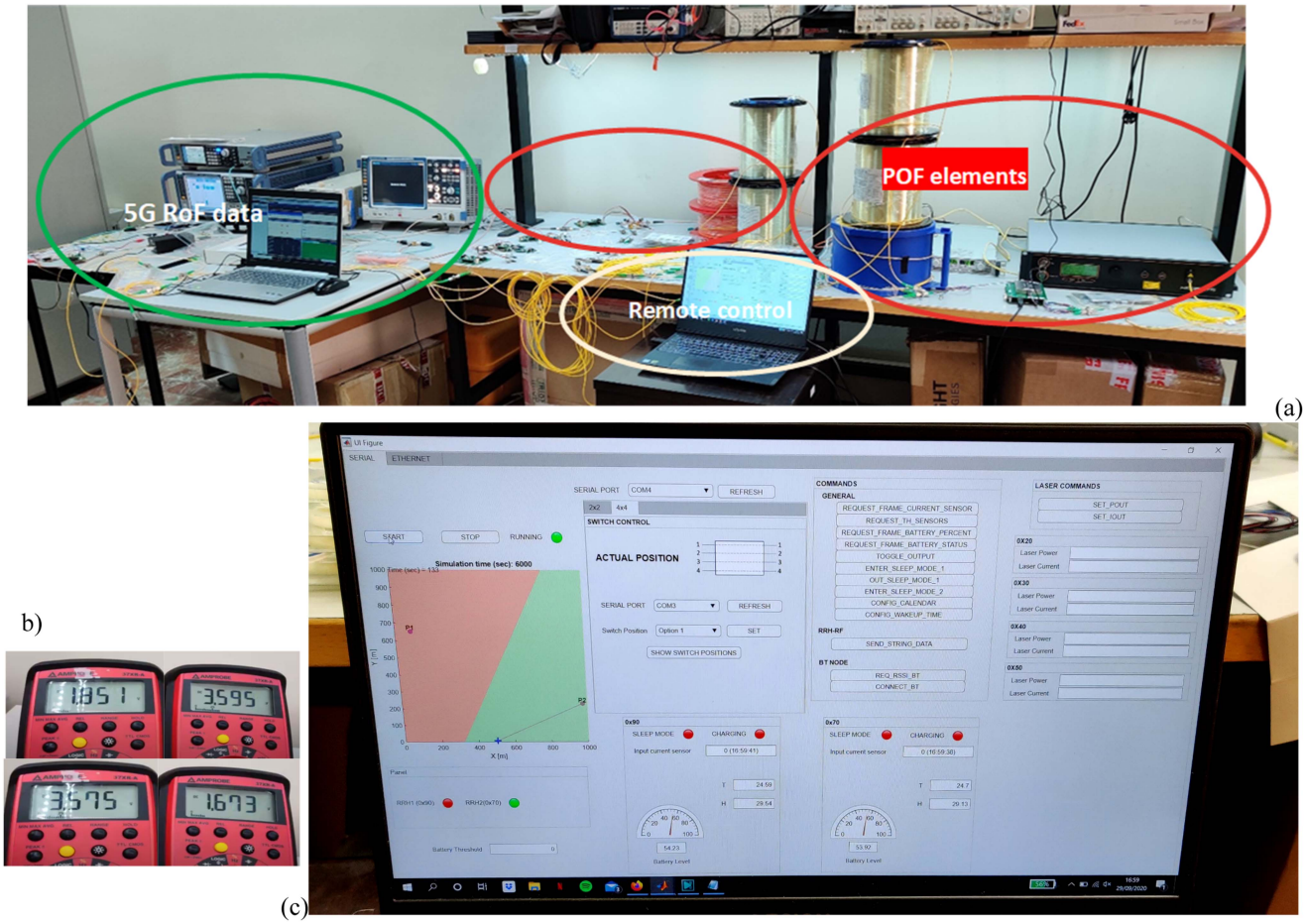

Fig. 5. (a) Experimental set-up on lab, (b) voltage measurements on PPC at RRH1 (left) and RRH2 (right), (c) mobility manager integration for PoF pooling operation.

The efficiencies of the PPCs were also calculated by measuring their PV curves. The obtained values were around 30%, slightly varying in each PPC. The efficiency of the DC/DC converters used to adapt the voltages generated by the PPCs is ∼88%. Therefore, electrical powers of around 190 mW and 125 mW are supplied to RRH1 at 10 km and RRH2 at 15 km respectively. The input power at each fiber after optical switch is around 1.7 W but with a HPL linewidth of 0.5 nm so there is no expected impact of Stimulated Brioullin Scattering (SBS), see [21]. Stimulated Raman Scattering (SRS) in a dedicated scenario is also negligible, and can have a small impact less than 2% in a shared scenario with 1.7 W HPL at 1480 nm and data at 1552.8 nm for a 14.47 km link as shown in [20].

In terms of optical power transmission efficiency (OPTE), if we consider the input optical power at the input of the switch to include its insertion losses and the optical power just before the PPC we have an OPTE of around 30 and 20% for RRH1 and RRH2 respectively.

In the tests, there are 2 voltmeters for measuring at PPC of RRH1 and RRH2. Fig. 5 shows photographs of the experimental set-up (a) and voltage measurements (b) when mobility manager simulates user movement between 2 small cells under RRH1 and RRH2 coverage area with their respective batteries below threshold levels and consequently, according to Fig. 3(b), PoF energy follows the user and PPC input optical power drops and consequently output voltage when PoF energy is not available. Fig. 5(c) shows the interface of the Matlab application with mobility manager on the left.

In our current experimental test-bed we use long link lengths of 10 km and 15 km and a splitter 1×2 to emulate to have 2 different HPLs. In that situation we provide to the load a maximum electrical power of 190 mW. If we shorten the distance from 10 km to 1 km and use the 5 W HPL providing 37.5 dBm in a single input port of the 4×4 switch we can have an input power after the switch (that can stand those 5 W) of 36.1 dBm that after propagation through the fiber and being split to reach 8 PPCs can provide those 960 mW that were used in the simulations. By using 5 HPL of 5 W instead, each connected to one 4×4 SW up to 20 RRHs with an available power of 960 mW each can be considered being the parameters used in simulations reported in Section II for each set of 4 RRHs powered by each HPL with the SW in a 1×4 configuration.

The PoF pooling concept is also tested for 4-MCF and 7-MCF set ups. In this last case, 4 cores are used for powering RRH1 with 4 PPCs and 1 core for powering a simulated RRH2 made up of a green LED, the other 2 cores were used for control uplink

and control downlink. The integration with the mobility manager and PoF agent is performed through the optical switch placed at the CO. Again, the SW selects the RRH to be powered by light depending on the location of the user. Part of PoF pooling configuration, mobility manager and switching capability were also integrated with an ARoF link [18] and demo video is available at [39]. This configuration with 7-MCF can easily integrate the monitoring technique reported in [40] to provide a safer operation of the energy delivery.

The main programmable hardware elements able to provide the connection with the mobility manager and PoF agent are the optical switch and the control board of the CO. Meanwhile the main programmable hardware element able to make the RRH to get into sleep mode operation, or to provide the energy to the load to charge a battery is provided by the control board at RRH. The remote control of RRH and the monitoring of RRH parameters at CO is feasible through the communication boards at both sides. In order to check functionality, different basic control operations/tests were implemented such as:

1) HPL ON, core/fiber selection for power delivery.
2) Battery charging through PoF channel until PoF agent decides to change core/fiber depending on mobility manager.
3) Sending control data from RRH to CO and from CO to RRH,
4) Displaying parameters at CO such as battery status.
5) Controlling from CO to enter RRH in and out of sleep mode,
6) Showing power consumption of different elements at RRH on sleep and active mode.
7) Mobility manager and PoF agent integration and controlling through optical switch and control board at CO.

All those functionalities are provided through the Matlab application and control through serial port as previously shown.

IV. Conclusion

A new strategy for energy efficiency in future 6G mobile network exploiting sleep mode operation supported by power over fiber (PoF) and sharing optical feeding between femtocells is described. The overall system throughput over a continuous 24-hour period of user requests is simulated and improved by more than 3 times when activating femtocells by PoF. The improvement goes up to more than 9 times when PoF is assisted by rechargeable batteries. Experimental tests are performed with a 4×4 SW in a centralized configuration that follows simulated users' movement. The set-up includes sleep mode operation with power consumptions of 5.8 mW at RRH to reduce power consumption in idle periods.

Acknowledgment

The authors want to thank David Sánchez Montero for his support in equipment installation and set-up deployment.

References

[1] White Paper Energy Efficiency, "An IEEE 5G and beyond energy roadmap," 2020. [Online]. Available: FutureNetworks.ieee.org/Roadmap

[2] N. Chen and M. Okada, "Toward 6G Internet of Things and the convergence with RoF system," *IEEE Internet Things J.*, vol. 8, no. 11, pp. 8719–8733, Jun. 2021, doi: 10.1109/JIOT.2020.3047613.

[3] "3GPP A global initiative," 2023. [Online]. Available: https://www.3gpp.org/news-events/3gpp-news/partner-pr-6g

[4] C. J. Bernardo and M. A. Uusitalo, "European vision for the 6G network ecosystem," The 5G Infrastructure Association, Jun. 2021. [Online]. Available: https://zenodo.org/records/5007671

[5] S. Buzzi, C. -L. I, T. E. Klein, H. V. Poor, C. Yang, and A. Zappone, "A survey of energy-efficient techniques for 5G networks and challenges ahead," *IEEE J. Sel. Areas Commun.*, vol. 34, no. 4, pp. 697–709, Apr. 2016, doi: 10.1109/JSAC.2016.2550338.

[6] N. A. Chughtai, M. Ali, S. Qaisar, M. Imran, and M. Naeem, "Energy efficiency maximization in green energy aided heterogeneous cloud radio access networks," in *Proc. IEEE 91st Veh. Technol. Conf.*, 2020, pp. 1–6, doi: 10.1109/VTC2020-Spring48590.2020.9128743.

[7] X. Zhang et al., "Macro-assisted data-only carrier for 5G green cellular systems," *IEEE Commun. Mag.*, vol. 53, no. 5, pp. 223–231, May 2015, doi: 10.1109/MCOM.2015.7105669.

[8] A. Delmade et al., "Optical heterodyne analog radio-over-fiber link for millimeter-wave wireless systems," *IEEE J. Lightw. Technol.*, vol. 39, no. 2, pp. 465–474, Jan. 2021.

[9] L. Bogaert et al., "36 Gb/s narrowband photoreceiver for mmWave analog radio-over-fiber," *J. Lightw. Technol.*, vol. 38, no. 12, pp. 3289–3295, Jun. 2020, doi: 10.1109/JLT.2020.2968149.

[10] T. Umezawa, P. T. Dat, K. Kashima, A. Kanno, N. Yamamoto, and T. Kawanishi, "100-GHz radio and power over fiber transmission through multicore fiber using optical-to-radio converter," *J. Lightw. Technol.*, vol. 36, no. 2, pp. 617–623, Jan. 2018.

[11] J. D. Lopez-Cardona, R. Altuna, D. S. Montero, and C. Vazquez, "Power over fiber in C-RAN with low power sleep mode remote nodes using SMF," *J. Lightw. Technol.*, vol. 39, no. 15, pp. 4951–4957, Aug. 2021.

[12] H. R. D. Filgueiras et al., "Wireless and optical convergent access technologies toward 6G," *IEEE Access*, vol. 11, pp. 9232–9259, 2023.

[13] M. Matsuura, "Power-over-fiber using double-clad fibers," *J. Lightw. Technol.*, vol. 40, no. 10, pp. 3187–3196, May 2022, doi: 10.1109/JLT.2022.3164566.

[14] "5G-NR base station (BS) radio transmission and reception (3GPP TS 38.104 version 15.5.0 release 15)," 2019. [Online]. Available: https://www.etsi.org/deliver/etsi_ts/138100_138199/138104/15.05.00_60/ts_138104v150500p.pdf

[15] J. D. López Cardona, P. C. Lallana, R. Altuna, A. Fresno-Hernández, X. Barreiro, and C. Vázquez, "Optically feeding 1.75 W with 100 m MMF in efficient C-RAN front-hauls with sleep modes," *J. Lightw. Technol.*, vol. 39, no. 24, pp. 7948–7955, Dec. 2021.

[16] C. Algora et al., "Beaming power: Photovoltaic laser power converters for power-by-light," *Joule*, vol. 6, no. 2, pp. 340–368, Feb. 2022.

[17] S. Wang, H. Yang, Y. Qin, D. Peng, and S. Fu, "Power-over-fiber in support of 5G NR fronthaul: Space division multiplexing versus wavelength division multiplexing," *J. Lightw. Technol.*, vol. 40, no. 13, pp. 4169–4177, Jul. 2022, doi: 10.1109/JLT.2022.3159540.

[18] J. D. Lopez-Cardona et al., "Power-over-fiber in a 10 km long multicore fiber link within a 5G fronthaul scenario," *Opt. Lett.*, vol. 46, pp. 5348–5351, 2021.

[19] F. M. A. Al-Zubaidi, J. D. Lopez-Cardona, D. S. Montero, and C. Vazquez, "Optically powered radio-over-fiber systems in support of 5G cellular networks and IoT," *J. Lightw. Technol.*, vol. 39, no. 13, pp. 4262–4269, Jul. 2021.

[20] R. Altuna, J. D. López-Cardona, F. M. A. Al-Zubaidi, D. S. Montero, and C. Vázquez, "Power-over-fiber impact and chromatic-induced power fading on 5G NR signals in analog RoF," *J. Lightw. Technol.*, vol. 40, no. 20, pp. 6976–6983, Oct. 2022.

[21] C. Vázquez et al., "Multicore fiber scenarios supporting power over fiber in radio over fiber systems," *IEEE Access*, vol. 7, pp. 158409–158418, 2019.

[22] D. M. Marom, Y. Miyamoto, D. T. Neilson, and I. Tomkos, "Optical switching in future fiber-optic networks utilizing spectral and spatial degrees of freedom," *Proc. IEEE*, vol. 110, no. 11, pp. 1835–1852, Nov. 2022.

[23] Z. Tan, C. Yang, and Z. Wang, "Energy evaluation for cloud RAN employing TDM-PON as front-haul based on a new network traffic modeling," *J. Lightw. Technol.*, vol. 35, no. 13, pp. 2669–2677, Jul. 2017, doi: 10.1109/JLT.2016.2613095.

[24] D. López-Pérez et al., "A survey on 5G radio access network energy efficiency: Massive MIMO, lean carrier design, sleep modes, and machine

learning," *IEEE Commun. Surveys Tuts.*, vol. 24, no. 1, pp. 653–697, First Quarter 2022, doi: 10.1109/COMST.2022.3142532.

[25] B. Debaillie, C. Desset, and F. Louagie, "A flexible and future-proof power model for cellular base stations," in *Proc. IEEE 81st Veh. Technol. Conf.*, 2015, pp. 1–7, doi: 10.1109/VTCSpring.2015.7145603.

[26] M. Deruyck, D. De Vulder, W. Joseph, and L. Martens, "Modelling the power consumption in femtocell networks," in *Proc. IEEE Wireless Commun. Netw. Conf. Workshops*, 2012, pp. 30–35, doi: 10.1109/WCNCW.2012.6215512.

[27] N. Piovesan, A. Gambin, M. Miozzo, M. Rossi, and P. Dini, "Energy sustainable paradigms and methods for future mobile networks: A survey," *Comput. Commun.*, vol. 119, pp. 101–117, 2018, doi: 10.1016/j.comcom.2018.01.005.

[28] Ericsson Presentation, 2019. [Online]. Available: https://mediabank.ericsson.net/deployedFiles/ericsson.com/Taking%20the%20next%20step%20in%20the%20indoor%20revolution.pdf

[29] G. Otero et al., "SDN-based multi-core power-over-fiber (PoF) system for 5G fronthaul: Towards PoF pooling," in *Proc. 44th Eur. Conf. Opt. Commun.*, 2018, pp. 1–3.

[30] R. Muñoz et al., "Experimental demonstration of advanced service management in SDN/NFV front-haul networks deploying ARoF and PoF," in *Proc. 45th Eur. Conf. Opt. Commun.*, 2019, pp. 459–463.

[31] WolframMathWorld, "Voronoi diagram," CoRR J. Sel. Areas Commun, 2024. [Online]. Available: http://mathworld.wolfram.com/VoronoiDiagram.html

[32] H. Elshaer, F. Boccardi, M. Dohler, and R. Irmer, "Downlink and uplink decoupling: A disruptive architectural design for 5G networks," in *Proc. IEEE Glob. Commun. Conf.*, 2014, pp. 1798–1803.

[33] N. Sapountzis, T. Spyropoulos, N. Nikaein, and U. Salim, "Optimal downlink and uplink user association in backhaul-limited HetNets," in *Proc. 35th Annu. IEEE Int. Conf. Comput. Commun.*, 2016, pp. 1–9.

[34] F. Boccardi et al., "Why to decouple the uplink and downlink in cellular networks and how to do it," *IEEE Commun. Mag.*, vol. 54, no. 3, pp. 110–117, Mar. 2016, doi: 10.1109/MCOM.2016.7432156.

[35] G. O. Pérez, A. Ebrahimzadeh, M. Maier, J. A. Hernández, D. L. López, and M. F. Veiga, "Decentralized coordination of converged tactile internet and MEC services in H-CRAN fiber wireless networks," *J. Lightw. Technol.*, vol. 38, no. 18, pp. 4935–4947, Sep. 2020, doi: 10.1109/JLT.2020.2998001.

[36] Q. Ye, B. Rong, Y. Chen, M. Al-Shalash, C. Caramanis, and J. G. Andrews, "User association for load balancing in heterogeneous cellular networks," *IEEE Trans. Wireless Commun.*, vol. 12, no. 6, pp. 2706–2716, Jun. 2013.

[37] COMBO (COnvergence of fixed and Mobile BrOadband access/aggregation networks), "Analysis of transport network architectures for structural convergence-D3.3," Jun. 2015. [Online]. Available: http://www.ict-combo.eu/data/uploads/deliverables/combo_d3.3_pu.pdf

[38] K. Smiljkovikj, L. Gavrilovska, and P. Popovski, "Efficiency analysis of downlink and uplink decoupling in heterogeneous networks," in *Proc. IEEE Int. Conf. Commun. Workshop*, London, U.K., 2015, pp. 125–130, doi: 10.1109/ICCW.2015.7247166.

[39] "PoF demo," 2021. [Online]. Available: https://www.youtube.com/watch?v=cbaZO5paKI8&t=23s

[40] R. Altuna, J. D. López-Cardona, and C. Vázquez, "Monitoring of power over fiber signals using intercore crosstalk in ARoF 5G NR transmission," *J. Lightw. Technol.*, vol. 41, no. 23, pp. 7155–7161, Dec. 2023, doi: 10.1109/JLT.2023.3300184.